

A Compliant Tactile Display for Teletaction *

G. Moy, C. Wagner, R.S. Fearing
Department of EE&CS
University of California
Berkeley, CA 94720-1770

Abstract

A teletaction system uses a tactile display to present the user with information about texture, local shape, and/or local compliance. Current tactile displays are flat and rigid, and require precise machining and assembly of many parts. This paper describes the fabrication and performance of a one-piece pneumatically-actuated tactile display molded from silicone rubber. Tactor spacing is 2.5 mm with 1 mm diameter tactor elements. Tactile display compliance ensures contact between the finger and tactile display at all times. Unlike previous pneumatic tactile displays, there is no chamber leakage and no seal friction. A psychophysics experiment showed that a synthetic grating on the tactile display was perceived as well as a low-pass-filtered real contact.

1 Introduction

The goal of a haptic interface is to realistically stimulate the user so that they feel like they are making contact with the actual environment. Haptic feedback can be broken down into two components, kinesthetic feedback and tactile feedback. Kinesthetic feedback systems are well developed compared to the current tactile feedback, also known as teletaction, systems. In teleoperation tasks, such as telesurgery, tactile feedback is an important addition to force feedback. A teletaction system provides information about texture, local compliance, and local shape which complements the force feedback system. An ideal teletaction system provides the user with a pattern indistinguishable from direct contact.

An ideal tactile display requires an actuator density of 1 per mm², with up to 2 mm indentation and 1 N of force per tactor, and a bandwidth > 50 Hz; that is, a power density of 10 W/cm². The performance requirements are a result of the 70 SA I mechanoreceptors per cm² [Johansson and Vallbo 1979] and force and displacement for compression of the finger [Serina et al 1997]. Tactile display designs have used solenoids [Fischer et al 1995], shape memory alloy [Howe et al 1995; Wellman et al 1997; Hasser and Daniels 1996], pneumatics [Cohn et al 1992; Caldwell et al 1999],

and MEMS [Ghodssi et al 1996]. Voice coil actuators have also been used [Pawluk et al 1998], but result in a large apparatus. Electrocutaneous stimulation [Kaczmarek et al 1991] is mechanically quite simple; however, the perceptual effects are hard to analyze. Typically, tactile displays control either displacements or forces. In a displacement display, an array of pins is shaped into a contour. In a force display, the pin array will produce a surface stress distribution representing the data. The tactile display's spatial density is limited by actuator size. Currently, the spacing between the centers of the pins is around 2 mm [Cohn et al 1992; Howe et al 1995].

In this paper, we present a compliant pneumatically actuated tactile display. The advantages of this compliant tactile display over previous pneumatically actuated tactile displays include conformability to the finger, no leakage, and no pin friction. Our display is easily fabricated by molding as a single part with no leakage. In a pin display, pin friction is dependent on side loading, which causes binding. A flat tactile display using pins for stimulation does not guarantee contact with the finger at all displacement levels. Pneumatically actuated pin displays have to overcome static friction whenever there is a change in force or displacement. Other pneumatic displays have problems with leakage, as seals would introduce too much friction.

We compare our display to the current state of the art portable tactile display [Caldwell et al 1999]. Caldwell has a tactile display which has 4 × 4 elements with 1.75 mm spacing, proportional filling valves, solenoid exhaust valves, high frequency texture valves, closed loop control, and an 11 Hz working frequency. Our display has 5 × 5 elements, uses only one binary valve per element, and has a working frequency of 5 Hz. Our design uses one binary valve per element because binary valves are easier to miniaturize and work well at tracking sinusoids with PWM control. With the no-leak design, we can use smaller valves which will lead to an integrated tactile display with the valves molded into the display. We plan to mold a tactile glove once miniature actuator technology is available.

We present the design and fabrication of a compliant pneumatically actuated tactile display in Section 2. We discuss the static performance in Section 3. We describe possible teletaction system designs in Sec-

*This work was funded in part by: NSF-PYI grant IRI-9157051 and NSF grant IRI-9531837.

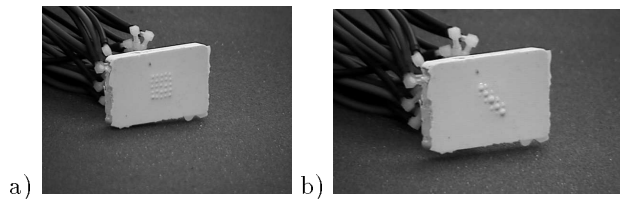


Figure 1: A 5×5 chamber array with a) all chambers inflated and b) a diagonal pattern inflated.

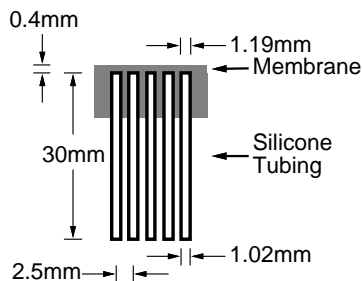


Figure 2: Cross section of the contact interface.

tion 4. We conduct a psychophysics experiment to determine the effectiveness of the tactile display in Section 4.

2 Design and Fabrication

The tactile display consists of two parts, the contact interface and the pneumatic valve array. The tactile display is designed to stimulate the SA I mechanoreceptors and consists of a 5×5 array of tactor elements (Figure 1). The elements are spaced 2.5 mm apart and are 1 mm in diameter, as seen in the cross section (Figure 2). The effective contact area is 25 mm^2 in a $12 \text{ mm} \times 12 \text{ mm}$ area. Instead of an array of actuated pins, we use an array of pressurized chambers as the stimuli. The enclosed pressurized chamber design ensures no extraneous stimuli from air leakage.

2.1 Contact Interface

The contact interface is molded from silicone rubber (HS II by Dow Corning) in a one-step process. The mold is shown in Figure 3. Twenty-five stainless steel pins (diameter 1.19 mm) extend 30 mm from the baseplate of the mold and are soldered to the back of the baseplate. The pins are planarized with the contact interface mold by a milling machine.

Silicone tubing (inner/outer diameter = 1.02/2.16 mm) is placed around each of the pins. The tubing does not extend to the end of the pins. The chamber size is determined by the diameter of the pin. The membrane thickness of the chambers is precisely controlled by spacers between the baseplate structure and contact interface mold. We use 0.4 mm of brass shim which leads to a membrane thickness of 0.4 mm. The spacing between elements is kept uniform by the contact interface mold.

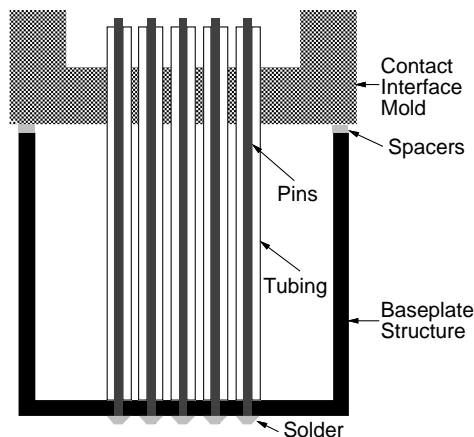


Figure 3: The contact interface mold used in fabrication.

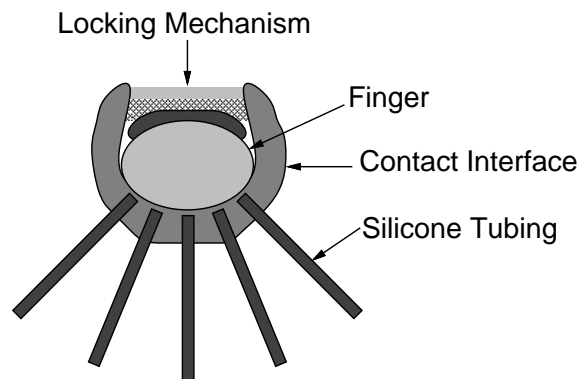


Figure 4: The contact interface wrapped around the finger with a locking mechanism above the fingernail.

The silicone rubber is poured into the mold and the mold is pressed against a flat surface. It takes 24 hours for the silicone rubber to cure. The silicone rubber bonds with the silicone tubing to form an airtight chamber. The flexibility of the contact interface provides constant contact between all the tactors and the finger (Figure 4). Since the tactile display is always in contact with the finger, we do not worry about a dead zone before the elements make contact. Attachment force of the contact interface to the finger can be controlled. The contact interface is connected to the pneumatic valve array by hoses and barbed connectors.

2.2 Valve Array

To control the pressure in each chamber, we use 25 Clippard solenoid 3-way valves [Cohn et al 1992]. A pulse width modulated (PWM) square wave controls the pressure in the chamber. The drawback of using PWM control is that the pressure in the chamber will always be vibrating at the PWM frequency. This vibration translates to a tactile 'buzz' felt by the finger and an audible 'buzz' that arises from the valve array. The magnitude of the PWM vibration will decrease

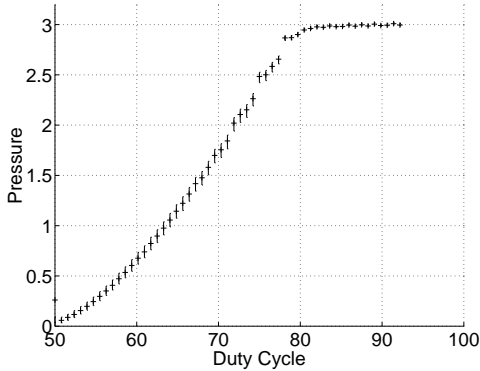


Figure 5: Chamber pressure vs. duty cycle. PWM frequency is 90 Hz. There is added capacitance between the valve and chamber to reduce PWM buzz. Residual feedthrough is shown as a vertical line. The valve is driven by a ± 20 volt supply, thus a 50% duty cycle is off.

with higher frequencies because the pressure change in one period will be smaller before the valve reverses direction. The drawback of using higher frequencies is the smaller range of usable duty cycles.

We reduce the buzz by adding a capacitance between the valve and contact interface. We use a capacitance of 11 cm^3 which leads to a RC time constant of 200 ms and a 3 db point at 5 Hz [see Cohn et al 1992 for calculations]. We change the duty cycle of the PWM square wave from 50% to 92% and measure the pressure at the inlet to the contact interface. The valve output pressure vs. duty cycle of the PWM wave is shown in Figure 5. The valve output pressure is not a linear function of duty cycle. With this characterization of the valve, a lookup table and interpolation can be used to compensate for the non-linearity. The useful range of duty cycles for a 90Hz PWM frequency is 50% to 80%.

We use a PWM frequency of 90 Hz, giving a good range of usable duty cycles and only moderate PWM buzz (Figure 5). To measure the dynamic performance of the valves, we controlled a valve to track a 1, 2, and 5 Hz sinusoid at a PWM frequency of 90 Hz. (Figure 6).

3 Static Performance

To measure the uniformity of the display and the quality of the manufacturing process, pressures of 2 to 4 atm are applied to the chambers. The corresponding displacement of the display is measured for each pressure and chamber. The displacement is determined using a mounted micrometer, adjusted to the point of contact with the display. The results are shown in Figure 7. At each pressure, the variation between chambers is about 15% from the average value.

Because the thickness of the membrane is the main variable between chambers, the uniform displacement distribution also demonstrates the regularity of the manufacturing process. The process is thus shown

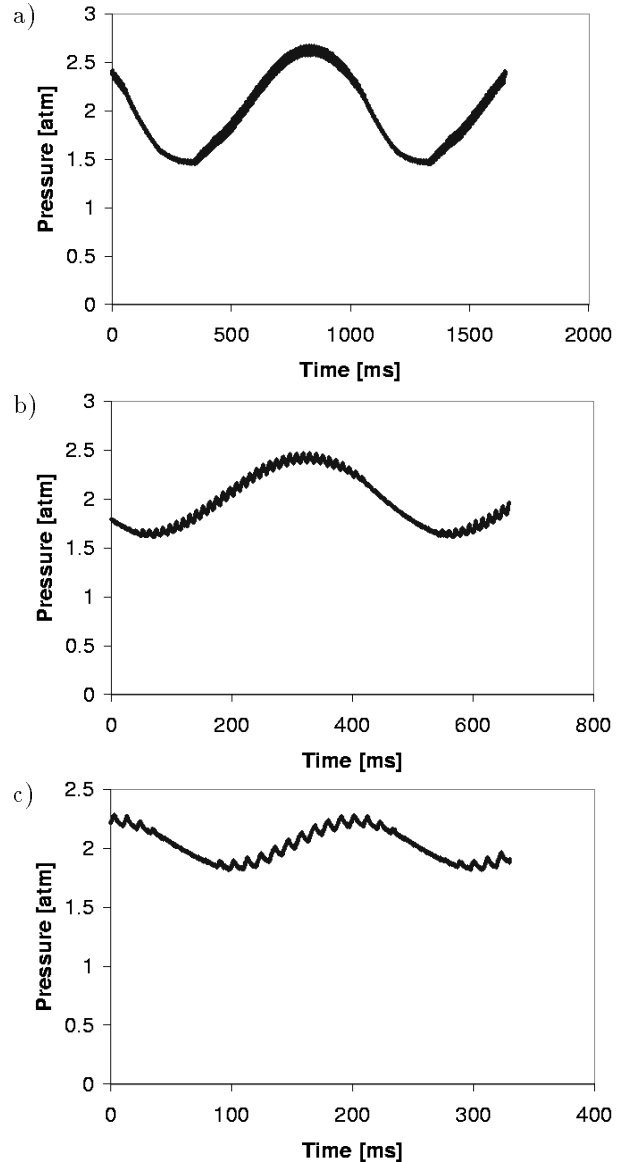


Figure 6: Tracking a a) 1 Hz, b) 2 Hz, and c) 5 Hz sinusoidal pressure function with a valve using a 90 Hz PWM frequency.

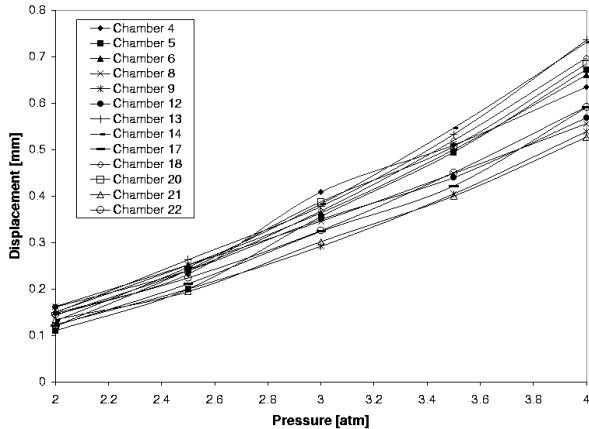


Figure 7: Uniformity test results.

to provide a uniform membrane thickness over every chamber. We are assuming that the material itself is uniform, as any inconsistencies in the rubber are minor compared to slight imperfections in the mold and molding process. If the spread of 15% is too high and the manufacturing process cannot easily be refined, the fidelity can be improved in software. Using a simple characterization, the variations can be corrected by a calibration matrix.

The force vs. displacement curves for 0.5 to 4 atm of pressure in 0.5 atm steps is measured and determines a complete mapping of supply pressure, force, and displacement. One representative chamber is used for the characterization because of the high similarity between chambers. The force at various displacements is determined by mounting a force/torque sensor on a micrometer driven stage, which has an accuracy of 0.001 mm along the axis of expansion of the display. The stage is set to a given displacement and a static supply pressure is applied to the chamber. The force is read from the force/torque sensor. This procedure is repeated for the range of displacements and pressures. The results are shown in Figure 8.

The intervals between curves are uniformly expanding. Various factors contribute to the non-linearity of the difference between curves, such as Hertzian contact between the chamber and force/torque sensor, and the nonlinear expansion of a rubber hemispherical membrane. With this force vs. displacement data, control software can compensate for such non-linearities.

For each static supply pressure, the force vs. displacement curve is linear. This conclusion is the most important consideration, because the tactile display cannot be fixed at a certain force or displacement across all users due to the differences in stiffness of the finger pad. Due to the linearity of the individual curves, the same information can be transmitted regardless of the indentation and placement of the individual finger. Note that pneumatic-driven pin dis-

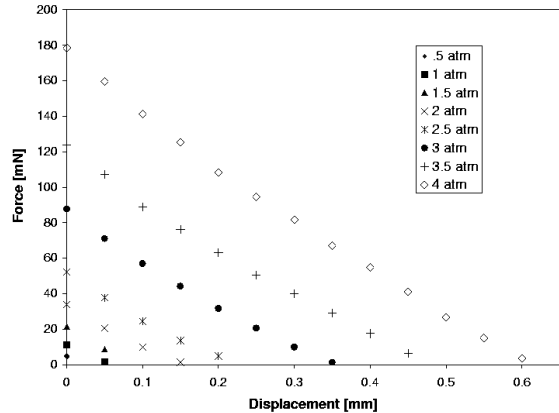


Figure 8: Force vs. displacement at various pressures.

plays [Cohn et al 1992; Caldwell et al 1999] are pure force displays, and that the shape memory alloy display of Wellman et al [1997] is closer to a displacement display due to its high inherent stiffness.

4 Tactile Display and Human Performance

A teletaction system consists of three main components, a tactile sensor, a tactile filter, and a tactile display. One application of a teletaction system is in a robotic laparoscopic telesurgery system [Tendick et al 1998]. The tactile sensor is mounted on the laparoscopic instrument (Figure 9), and the tactile display is mounted on the master manipulator. The tactile filter converts the sensor data (typically normal strain for a capacitive sensor [Fearing 1990]) to force, displacement, or pressure data for the tactile display. The conversion problem is formulated as a stress matching problem as seen in Figure 10 [Fearing et al 1997].

In stress matching, we attempt to match boundary conditions (stress profiles) at depth $d/2$. With matched boundary conditions, the stresses on the finger surface are as close to the real contact stresses as possible. If the spatial frequency of the tactile elements is high enough and the pressures are exact, the tactile display will realistically represent an actual contact through elastic lowpass filters. An ideal tactile display would generate a pattern of normal stress on the reconstruction filter layer which is equivalent to the sensed stress at a depth $d/2$ in the tactile sensor. Our actual display generates mostly normal stress on the finger or reconstruction layer, with some slight shear stress due to surface friction. Previous work by Moy et al [2000] has quantified the amplitude resolution of the human tactile system for low-pass filtered gratings, and provides guidance for how accurately the tactile display stresses need to be controlled to convey the same information as a real contact.

To test the performance of the tactile display, we



Figure 9: A tactile sensor mounted on a laparoscopic instrument, and components including (top to bottom) molded dielectric, upper copper layer, circuit board, and mount.

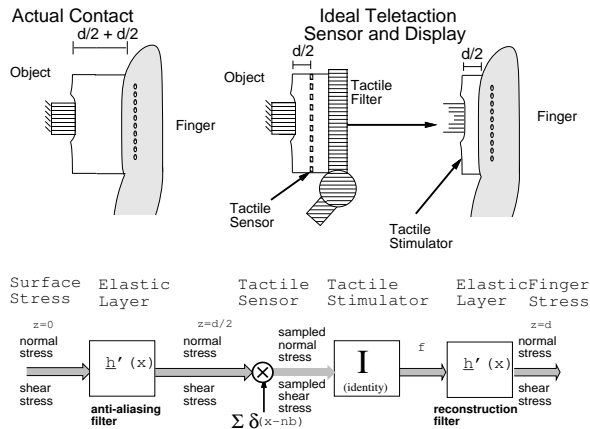


Figure 10: Stress matching for teletaction systems.

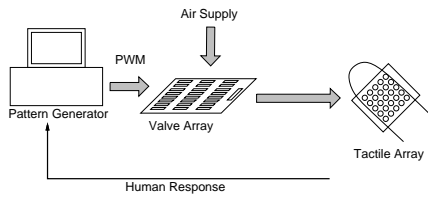


Figure 11: Test apparatus.

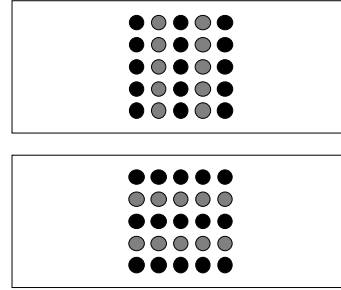


Figure 12: The vertical and horizontal grating patterns used as stimuli. Black dots indicate full pressure. Grey dots indicate 20%, 34%, 50%, 69% or 90% of full pressure.



Figure 13: The tactile display attached to the finger.

conduct a psychophysics experiment using simulated gratings, with a 5 mm period. We can then directly compare the results with contacts with real gratings. In the experiment, subjects are asked to determine the direction of a grating pattern presented to them on the tactile display. The apparatus is shown in Figure 11.

We generate simulated square gratings with 5 mm period in horizontal and vertical orientations as shown in Figure 12. The grating troughs are at 20%, 34%, 50%, 69% or 90% of the grating peak pressure of 3 atm. The experiment consists of presenting 300 patterns to each subject. The 300 patterns consist of 30 grating patterns in each orientation at five different trough pressure levels. The experiment is broken down into 6 sessions of 50 trials each.

The tactile display is secured to the subject's finger with two wires wrapped around the display and finger (Figure 13). The grating pattern is presented for 3 seconds and the subject is given an additional 3 seconds to respond. One second of rest is given after the response is recorded. Subjects listen to white noise through headphones to remove audio cues from the valve array.

The experiment was conducted on 6 voluntary subjects with no known impairments in tactile sensory functions. The raw data is shown below. The average

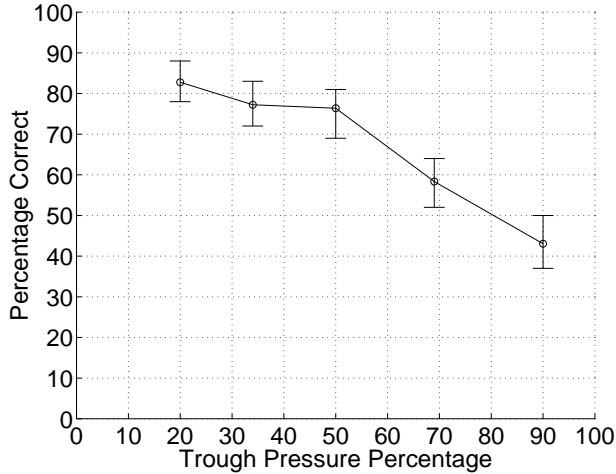


Figure 14: Results of the psychophysics experiment with 95% confidence intervals [Natrella 1963].

results are shown in Figure 14.

| Subject | 90% | 69% | 50% | 34% | 20% |
|---------|-----|-----|-----|-----|-----|
| 1 | 15 | 32 | 47 | 49 | 56 |
| 2 | 26 | 41 | 48 | 47 | 46 |
| 3 | 24 | 34 | 45 | 44 | 52 |
| 4 | 29 | 30 | 47 | 47 | 50 |
| 5 | 36 | 31 | 41 | 42 | 43 |
| 6 | 25 | 42 | 47 | 49 | 51 |

We compare these results with previous results shown in Figure 15 [Moy et al 2000]. We convert the results to use the modulation index, defined as:

$$\sigma_z(x) \sim \alpha_\sigma(1 + \mu_\sigma \cos(\omega x))$$

where $\sigma_z(x)$ is the applied normal stress profile, α is the scaling factor, μ_σ is the modulation index, and ω is the frequency of the grating. The converted results are shown in Figure 16. Our results correlate well with previous data. The just noticeable difference point is approximately 0.1 modulation index units (a 10% amplitude variation). As the modulation index gets higher (trough pressures get lower), the perception of grating orientation also gets higher. We thus conclude that our tactile display has sufficient amplitude resolution to match human perceptual limits.

5 Conclusions and Future Work

We have developed a compliant tactile display which remains in contact with the finger at all times. The fabrication process is a one-step mold. The molding process has accurate control of membrane thickness. Silicone tubing from the contact interface gives easy access to connections with the Clippard valve array. Better and more consistent connections are needed since one of the connections popped out with only 3 atm of pressure. Without the finger contact, each chamber can withstand at least 4 atm of pressure. Burst pressure without contact varies from 5 to 6 atm.

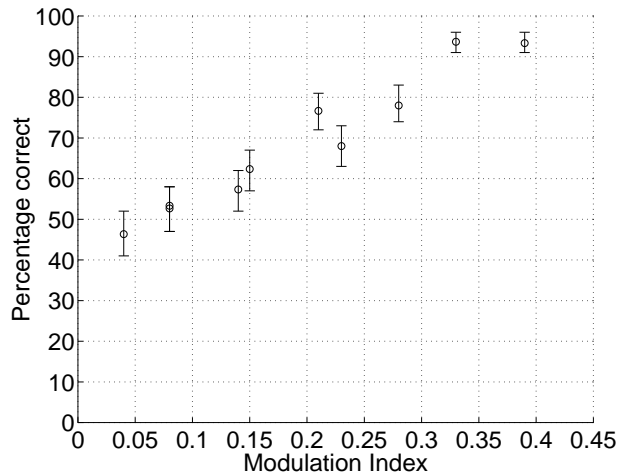


Figure 15: Results from previous psychophysics experiments relating grating orientation perception and modulation index for contacts with machined wax blocks [Moy et al 2000]. Error bars represent 95% confidence intervals for $n=300$.

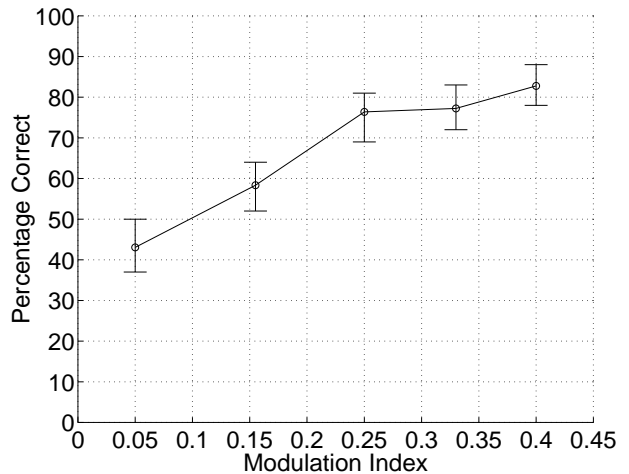


Figure 16: Results from the psychophysics experiment relating grating orientation perception and modulation index for the compliant tactile display. Error bars represent 95% confidence intervals for $n=360$.

A basic psychophysics experiment shows that adequate tactile information is transmitted through the tactile display. The results of grating orientation detection experiment using the tactile display correlate well with previous grating orientation detection experiments using wax blocks as the stimuli [Moy et al 2000]. With a tuned valve array and better pneumatic connections, the tactile display can be run at higher pressures.

Future work includes:

- Integrate pressure sensors to each element
- Close the control loop
- Use smaller and faster valves to reduce weight and improve high frequency response
- Calibrate the tactile display to give higher fidelity and uniformity
- Use more robust tubing and connections
- Conduct more psychophysics studies to test the performance of the teletaction system

This tactile display is simple and inexpensive to fabricate. The tactile display is cheap enough to be disposable and easily customized for different sized fingers. The expensive fixed cost item is the 5×5 valve array, which in principle could be reduced to 1 cm^3 using MEMS technology. The required flow rate is quite low if the valve can be mounted close to the display. Hence, a portable, lightweight, comfortable tactile display will soon be possible. The ultimate goal is to manufacture a molded tactile display glove.

Acknowledgments

We thank John Lin for his early work on the tactile display, and K. Chiang, and J. Yan for helpful discussions and comments.

References

- [1] D. G. Caldwell, N. Tsagarakis, and C. Giesler, "An Integrated Tactile/Shear Feedback Array for Stimulation of Finger Mechanoreceptor", *IEEE Int. Conf. Rob. and Auto.*, vol. 1, pp. 287-292, Detroit, MI, May 1999.
- [2] M. B. Cohn, M. Lam, and R. S. Fearing, "Tactile Feedback for Teleoperation", *SPIE Telemat. Tech.*, vol. 1833, pp. 240-254, Boston, MA, November 15-16, 1992.
- [3] R. S. Fearing, "Tactile Sensing Mechanisms", *Int. Jnl. of Robotics Research*, vol. 9, no. 3, pp. 3-23, June 1990.
- [4] R. S. Fearing, G. Moy and E. Tan, "Some Basic Issues in Teletaction", *IEEE Int. Conf. Rob. and Auto.*, vol. 4, pp. 3093-9, Albuquerque, NM, 20-25 April 1997.
- [5] H. Fischer, B. Neisius, and R. Trapp, "Tactile Feedback for Endoscopic Surgery" in *Interactive Technology and New Paradigm for Healthcare*, edited by K. Morgan, R. M. Satava, H. B. Sieburg, R. Mattheus, J. P. Christensen, pp. 114-117, IOS Press 1995.
- [6] R. Ghodssi, D. J. Beebe, V. White, and D. D. Denton, "Development of a Tangential Tactor Using a LIGA/MEMS Linear Microactuator Technology", *1996 Int. Mech. Eng. Cong. and Exposition, Microelectromechanical Systems*, DSC Vol. 59, pp. 379-386, Nov. 17-22, 1996.
- [7] C. J. Hasser and M. W. Daniels, "Tactile Feedback with Adaptive Controller for a Force-Reflecting Haptic Display", *15th Southern Biomedical Engineering Conf.*, pp. 526-533, Dayton, OH, March 29-31, 1996.
- [8] R. D. Howe, W. J. Peine, D. A. Kontarinis, and J. S. Son, "Remote Palpation Technology", *IEEE Eng. in Med. and Bio. Mag.*, pp. 318-323, May/June 1995.
- [9] Johansson, R. S. and Vallbo, A. B. "Detection of Tactile Stimuli. Thresholds of Afferent Units related to psychophysical thresholds in the human hand", *J. Physiology*, vol. 297, pp. 405-422, 1979.
- [10] K. A. Kaczmarek, J. G. Webster, P. Bach-y-Rita, and W. J. Tompkins, "Electrotactile and Vibrotactile Displays for Sensory Substitution Systems", *IEEE Trans. on Biomedical Engineering*, vol. 38, no.1, pp. 1-16, Jan. 1991.
- [11] G. Moy, U. Singh, E. Tan, R. S. Fearing, "Human Psychophysics for Teletaction System Design", to appear in *Haptics-e: The Electronic Journal of Haptics Research*, 2000.
- [12] M.G. Natrella, *Experimental Statistics*, Department of Commerce, National Bureau of Standards, 1963.
- [13] D. T. V. Pawluk, C. P. van Buskirk, J. H. Killebrew, S. S. Hsiao, and K. O. Johnson, "Control and Pattern Specification for a High Density Tactile Array", *IMECE Proc. of the ASME Dyn. Sys. and Control Div.*, vol. 64, pp. 97-102, Anaheim, CA, November 1998.
- [14] Serina, E. R., Mote, C. D., Jr., and Rempel, D., "Force response of the fingertip pulp to repeated compression-effects of loading rate, loading angle and anthropometry", *J. Biomechanics*, vol.30, (no.10), pp. 1035-40, Oct. 1997.
- [15] Shimojo, M., Shinohara, M., and Fukui, Y., "Human Shape Recognition Performance for 3-D Tactile Display", *IEEE Trans. on Systems, Man, and Cybernetics, Part A: Systems and Humans*, vol. 29, no. 6, pp. 637-644, November 1999.
- [16] Tendick, F., Sastry, S. S., Fearing, R. S., and Cohn, M., "Applications of Micromechatronics in Minimally Invasive Surgery", *IEEE/ASME Trans. on Mechatronics*, vol. 3, no.1, pp. 34-42, March 1998.
- [17] Wellman, P. S., Peine, W. J., Favallora, G., and Howe, R. D., "Mechanical Design and Control of a High-Bandwidth Shape Memory Alloy Tactile Display", *Int. Symp. on Experimental Robotics*, pp. 56-66, Barcelona, Spain, June 1997.